Vision Research 69 (2012) 42–48

Contents lists available at SciVerse ScienceDirect

Vision Research

journal homepage: www.elsevier.com/locate/visres

Photopic and scotopic multifocal pupillographic responses in age-related macular degeneration

Y. Rosli [a,b], S.M. Bedford [b], A.C. James [b], T. Maddess [b,*]

[a] Program of Biomedical Science, School of Diagnostic and Applied Health Sciences, Faculty of Health Sciences, Universiti Kebangsaan Malaysia, Jalan Raja Muda Abdul Aziz, Kuala Lumpur, Malaysia

[b] The ARC Centre of Excellence in Vision Science, John Curtin School of Medical Research, Australian National University, Canberra, ACT 0200, Australia

ARTICLE INFO

Article history:
Received 29 April 2012
Received in revised form 23 July 2012
Available online 7 August 2012

Keywords:
Multifocal pupillography
Age-related macular degeneration
Photopic
Scotopic
Pedestal flicker

ABSTRACT

We compared photopic and scotopic multifocal pupillographic stimuli in age-related macular degeneration (AMD). Both eyes of 18 normal and 14 AMD subjects were tested with four stimulus variants presented at photopic and 126 times lower luminances. The multifocal stimuli presented 24 test regions/eye to the central 60°. The stimulus variants had two different check sizes, and when presented either flickered (15 Hz) for 266 ms, or were steady for 133 ms. Mean differences from normal of 5 to 7 dB were observed in the central visual field for both photopic and scotopic stimuli (all $p < 0.00002$). The best areas under receiver operating characteristic plots for exudative AMD in the photopic and scotopic conditions were 92.9 ± 8.0 and 90.3 ± 5.7% respectively, and in less severely affected eyes 83.8 ± 9.7% and 76.9 ± 8.2%. Damage recorded at photopic levels was possibly more diffusely distributed across the visual field. Sensitivity and specificity was similar at photopic and scotopic levels.

1. Introduction

Age-related macular degeneration (AMD) has been estimated to affect between 0.7% and 1.9% of the population (Mitchel, Smith, & Altebo, 1995; VanNewkirk et al., 2000). The disease leads to photoreceptor death, primarily in the macula. Rod function may be diminished earlier than cone function in early AMD (Curcio, Medeiros, & Millican, 1996; Curcio et al., 1993; Curcio, Owsley, & Jackson, 2000; Jackson, Owsley, & Curcio, 2002; Owsley et al., 2000; Scholl et al., 2004). That being said early loss of cone function and structural integrity has also been reported (Shelley et al., 2009; Smith, Pokorny, & Diddie, 1988), and changes in parameters related to dark adaptation have better diagnostic power for cones than for rods (Dimitrov et al., 2008, 2012) as well as better reproducibility (Dimitrov et al., 2011). Neelam et al. (2009) provide and excellent review of psychophysical testing in AMD.

Standard electrophysiology methods have provided inconsistent results in AMD (Gerth, 2009). We have shown that a 64 electrode multifocal VEP, that concurrently presented 88 regions per eye, had considerable diagnostic power for AMD (Rosli et al., 2009), but the method requires lengthy set-up time. More recently we have developed multifocal pupillographic objective perimetry (mfPOP), which has shown high sensitivity and specificity for glaucoma (Carle, James, et al., 2011; James et al., 2011; Maddess et al., 2009) and early-stage diabetic retinopathy (Bell et al., 2010).

The issue of whether mfPOP has clinical utility in AMD has been partly addressed by studies using 44 photopic stimuli per eye presented to the central 30° that have produced %AUC values of 100 ± 0.0% for exudative AMD and even for early stage AMD (Sabeti et al., 2012; Sabeti, Maddess, & James, 2010). Two studies reported mfPOP quantifies recovery produced by ranibizumab treatment (Sabeti et al., 2011, 2012). Interestingly markers based on mfPOP pre-treatment results are predictive of post-treatment outcomes (Sabeti et al., 2012). Given the age demographic for AMD it is significant that a study on 162 subjects indicated that mfPOP appears not to be affected by lens replacement surgery for cataracts (Kolic et al., 2010). Taken together these studies indicate that mfPOP may have some clinical utility for AMD.

This study exploited an older version of the mfPOP hardware platform that allowed us to examine the relative diagnostic power of mfPOP at light levels where either rod or cone photoreceptors would dominate. To insure that rod dominated parts of the retina were probed the stimuli tested the central 60° of the visual field. Outcome measures include sensitivity, specificity, and the average disposition and depth of visual field defects.

2. Materials and methods

2.1. Subjects

Eighteen normal subjects had no history of eye diseases, best corrected acuity ⩽0.2 (logMAR), normal intraocular pressure and normal visual field on perimetry (FDT Perimeter, Welch Allyn,

* Corresponding author. Fax: +61 2 6125 9532.
E-mail address: ted.maddess@anu.edu.au (T. Maddess).

0042-6989/$ - see front matter © 2012 Elsevier Ltd. All rights reserved.
http://dx.doi.org/10.1016/j.visres.2012.07.019

Table 1A
Demographic data.

	N	Age mean ± SD	Age range	Female fraction
Normal	18	67.4 ± 9.02	58–80	0.50
AMD	14	75.5 ± 7.1	62–90	0.57

Tested eyes – Photopic: normal = 36, AMD = 28; Scotopic: normal = 34, AMD = 20.

USA). Their demographic data and those of the fourteen AMD patients are given in Table 1A. No subjects were pseudophakic, or had other eye surgery or history of eye disease, other than AMD in the patients. All subjects had both eyes tested concurrently with each of 8 mfPOP methods (see below) providing a total of $8 * 2 * (14 + 18) = 512$ visual fields. The patients' eyes were classified into three categories of disease severity (Sev1–Sev3) designed to give three roughly equal sized groups. When data from these severity groupings were analysed separately the statistical cost of using these smaller groups was indicated by providing standard errors in the resulting outcome measures. The objective was to have a range of disease severities to compare at photopic and scotopic conditions.

Grading was based on photos taken with dilated pupils using the 45° setting of a Zeiss Visucam$^{NM/FA}$ fundus camera, and a Cirrus macular OCT scan (both Carl Zeiss Meditech, Dublin, CA, USA). Given that at least one of the patients' eyes was quite affected (Table 1B) fluorescein angiography was also performed. Sev1 contained putatively normal fellow eyes of AMD patients, two each at logMAR 0 and 0.2. The Sev2 eyes had soft drusen or pigmentary changes and often some degree of geographic atrophy, three eyes had CF acuity and the remainder had median logMAR acuities of 0.39 ± 0.34 (range −0.1 to 1). Sev3 eyes had exudative AMD, five of these eyes having Seeing Fingers acuity (CF), 1 Hand Motion, 1 Light Perception, and the remainder had median (±SD) logMAR acuities of 0.48 ± 0.27 (range 0.3–1). None of the subjects had systemic diseases or were on medications known to affect retinal function, although most of the Sev3 eyes had been treated with ranibizumab. Although AMD is generally quite bilateral four of the subjects differed in their severities by 1 step, and two by 2 steps (Table 1B). All subjects gave informed written consent. This study was approved by ANU Human Research Ethics Committee (Protocol 04-238) and adhered to the tenets of the Declaration of Helsinki.

2.2. Stimuli and recording

Multifocal visual stimuli were presented using a prototype of the Truefield® Analyzer (TFA) (Seeing Machines Ltd., Australia). We recorded pupillary responses to independent stimulation of 24 stimulus regions/eye (dichoptic) within the central 60°. Each display presented a circular dart-board like ensemble of white stimuli with a small red fixation cross presented at the centre (Fig. 1). Pupil responses were recorded by video cameras at 30 frames/s under infrared illumination. The older hardware platform made it relatively easy to introduce neutral density filters, which reduced luminance levels by 125.9 times (ND = 2.1). Thus for photopic stimuli the background and maximum stimulus luminances were 10 and 150 cd/m^2; 0.08 and 1.2 cd/m^2 for the scotopic cases. For the scotopic stimuli all subjects were adapted to the

Table 1B
AMD severity by eye.

Patient	1	2	3	4	5	6	7	8	9	10	11	12	13	14
OS	3	3	1	3	3	3	2	3	2	3	2	3	2	3
OD	3	3	2	3	3	2	2	3	1	1	1	1	2	2

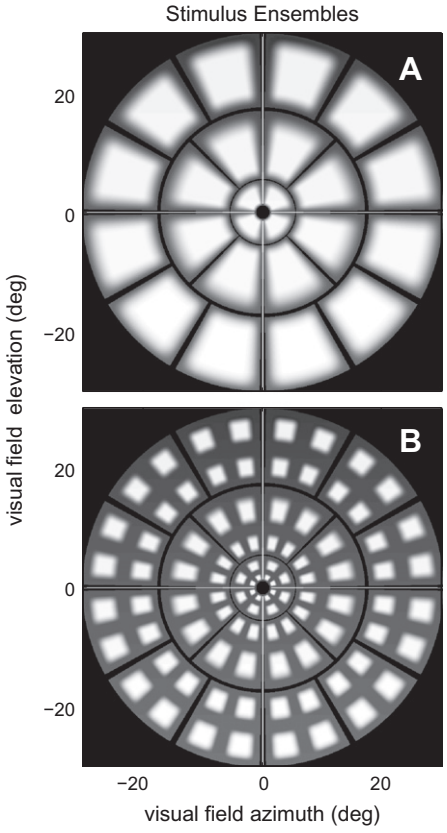

Fig. 1. Layout of test regions for scotopic stimulus condition used, shown as if all 24 regions were active simultaneously. (A) A one check/side stimulus; (B) a 2 check/side stimulus (cf. Table 2). For the sake of presentation the background of each region in (B) has been made brighter so that the boundaries of each stimulus regions are visible. No stimuli were presented to the central 1°, where a red fixation cross was presented. The outer borders of the stimuli were at 4.9°, 15.7° and 29.5° from fixation. Also visible in this figure are long lines presented along the meridians to aid fixation in AMD eyes and to aid in fusion of the dichoptic stimuli (vertical lines). Fixation was monitored online. The vertical lines also assist with maintain fusion of the left and right eye stimuli.

background luminance for 20 min. Otherwise the scotopic stimuli were the same as the photopic stimuli.

Four different stimulus methods (protocols) were repeated at the photopic and scotopic conditions Table 2, and see below. A large white cross spanning 60° of the field that was centred on fixation was also presented to help AMD subjects to fixate (Fig. 1A and B). The vertical line of that pair also assisted subjects to maintain fusion of the dichoptic stimuli. There was also a central fixation cross, which assisted fixation via healthier (fellow) eyes. All stimuli were 4 min in duration, presented in eight segments of 30 s. Segments only needed to be repeated if more than 15% of a

Table 2
Summary of the stimulus protocols.

Stimulus protocol	Checks/side	Flicker (Hz)	Duration (ms)
Photo1	1	0	133
Photo1F	1	15	266
Photo2	2	0	133
Photo2F	**2**	**15**	**266**
Scot1	1	0	133
Scot1F	**1**	**15**	**266**
Scot2	2	0	133
Scot2F	2	15	266

For photopic stimuli the background and maximum stimulus luminances were 10 and 150 cd/m^2, and for the scotopic stimuli 0.08 and 1.2 cd/m^2. The mean presentation rate of the stimuli was 1/s/region.

segment record was lost due to blinks and fixation losses, which were monitored online. The stimuli were blurred so that they contained no spatial frequencies above 1.5 cpd, and so refractive errors on the order of 2 D will not significantly reduce the contrast of the stimuli. Accordingly subjects' vision was corrected to the nearest 1.5 D spherical equivalent. The blurred skirts of the stimuli also reduced the effects of small fixation errors.

All the stimuli had a mean presentation rate of 1/s/region, i.e. 24 presentations/s/eye. When the stimuli were presented they either remained on for 133 ms or switched between the background and the test pattern (pedestal flickered) at 15 Hz for 266 ms. Since the duty cycle of the flicker was 50%, both the steady and flickered stimuli presented the same amount of light on each presentation. Given these factors the time-average luminance at each region was 0.23 and 28.0 cd/m^2 for the scotopic and photopic conditions. Some stimuli also had a 2 by 2 check/region pattern (cf. Fig. 1A and B), as used elsewhere (Maddess et al., 2009).

Assessing visual function at different eccentricities raises the issue of how the stimuli overlapped with the distribution of rods and cones at different retinal locations. The rod free zone extends to about 0.7°, the innermost stimuli here extended from 1° to 4.9° (Fig. 1 legend). The ratio of rods to cones is about 5 at 3.6° and rises to its maximum value of 20–30 by 14° (Curcio et al., 1990), remaining at those levels out to the maximum eccentricity examined here (29.5°). Thus the field examined here is rod dominated in normal persons.

2.3. Analysis

Estimates of the mean pupil responses for each region in the photopic and scotopic conditions were obtained by a multiple regression analysis (Bell et al., 2010; Maddess et al., 2009, 2011). We have shown that the noise in direct and consensual pupil responses is quite correlated and so rather than averaging these responses for a given retina it best to select the pupil giving the largest signal to noise ratio for each retina (Bell et al., 2010; Maddess et al., 2009, 2011). We followed that method here. This has the side benefit that only one pupil needs to be functioning well for the test to proceed. As in previous studies we did not use the absolute contraction amplitudes, instead the raw pupil record was first normalised to the middle value of a trend line through the data, and them multiplied by 3.5 mm to create standardised contraction amplitudes. This method greatly reduces the age dependence of the pupillary responses to mfPOP stimuli (Bell et al., 2010; Carle, James, et al., 2011; Maddess et al., 2009, 2011).

The response amplitudes for each region were transformed to decibels, which stabilized the variance. This also made the results more similar to those from standard perimetry and permitted pattern deviations (PDs) to be calculated as usual: subtracting the 86th percentile of the decibel total deviations (TDs) values. The TDs were the differences of the any given subject's decibel contraction amplitude results from the mean response at each visual field location of the normal subjects. There was also a small factor for gender included, which was highly significant (e.g. Table 5), and which has been found in our other studies. Receiver operator characteristic (ROC) analysis was used to quantify the diagnostic power of the eight methods in terms of percent area under the curve (AUC), sometimes presented as %AUC to improve readability. The total deviations (TDs) and pattern deviations (PDs) were converted to *Z*-scores before the ROC analysis (Bell et al., 2010; Maddess et al., 2009). Multivariate linear models were also used to explore which independent variables significantly determined the pupil response amplitudes.

3. Results

Examples of the independent responses to each stimulus region of the *Photo1* stimulus array (Table 2) are shown in Fig. 2. Given the mean presentation rate of 1/s/region, and the stimulus duration, one can think of each of these response waveforms as the average responses to 240 stimulus presentations. The patient had logMAR acuities of 0.2 OD and 1.0 OS. The reduced acuity was associated with reduced responses in the four central regions of the left eye.

3.1. ROC analysis

For each visual field the deviations (TDs and PDs) from the normative data were taken as the input to receiver operator characteristic (ROC) analyses. As reported previously (Bell et al., 2010; Carle, James, et al., 2011; James et al., 2011; Maddess et al., 2009; Sabeti et al., 2011, 2012), the ROC analysis was repeated 20 times begin-

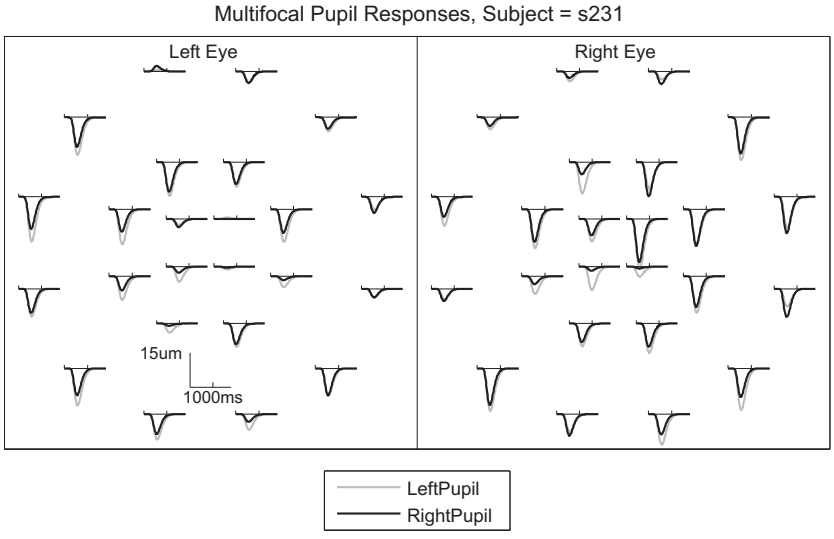

Fig. 2. Illustrations of the multifocal responses of an individual AMD patient recorded in response to the simplest photopic stimulus, *Photo1* (Table 2). There was an average of 240 presentations per region within the 240 s of the test period. The subject had exudative AMD in the left eye and non-exudative in the right. LogMAR visual acuities for the left and right eyes were 1.0 and 0.2 respectively. There is a marked reduction of the central 4 responses of the left eye. As indicated in the legend at bottom left pupil responses are shown in grey, right pupil in black. The plots also show the commonly reported feature of larger peripheral temporal field responses.

ning by considering only the single most deviating visual field region in each field (*N*-worst = 1), and then increasing the number of these *N*-worst regions to include: the two most deviating regions, three most deviating and so on up to the 20 worst deviations from normal (akin to ROC analysis on the mean defect). This allows methods that can detect focal lesions to be identified no matter where in the field the lesions occur. Fig. 3 shows the resulting AUC values as a function of the *N*-worst regions for the four best performing photopic and scotopic protocols. For all the methods and disease severities the 1st to 3rd-worst regions are generally the most diagnostic, indicating that the clinically significant damage is mainly localised rather than diffuse. Fig. 3 only shows data out to the worst 20 locations per field. When all 44 regions are considered this is like basing the ROC analysis on the mean defect, in all cases the AUC value for $N = 44$ was $\leqslant$the value for $N = 20$.

Table 3 summarises %AUC values for all eight protocols (see table legend for SE). To arrive at the tabulated values we took the mean of the %AUC for *N*-worst from 1 to 3, and then took the larger of the two %AUC obtained for either the TDs or PDs. This conservative method de-emphasised any spuriously high %AUC (for one of *N*-worst = 1–3). For photopic and scotopic fields *Photo2F* and *Scot1F* achieved the highest mean %AUCs (bold), either when all severities were pooled (All Sev), or when only more severe eyes were considered (Sev2 and 3 pooled). Performance of those two protocols as function of *N*-worst was shown by the solid lines in Fig. 3. We concentrated on those two protocols in our further analysis, since they were the most interesting clinically.

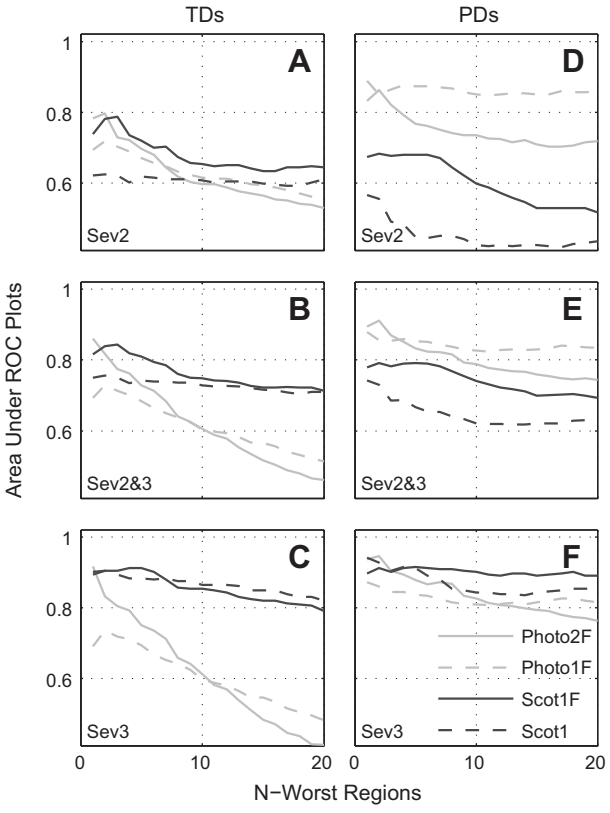

Fig. 3. Area under curve for AMD severities according to the number visual field regions that are most deviating from normal (*N*-worst). Results for the two best performing photopic and scotopic protocols (see Table 3). The photopic protocols have grey lines, scotopic back. The best performing method at each light level has a solid line, second best dashed (see legend in panel (F)). For most protocols the best AUC is reached by considering the worst 1–3 regions. PDs generally outperformed TDs for milder disease. Table 4 gives means and SEs for the mean of the first three *N*-worst. (B) and (D) include all AMD eyes and normal eyes.

Table 3
Percent areas under curve (AUC) for all the stimulus protocols. The two columns are figures when patient eyes of all severities of AMD are compared with normals (All Sev), and just Sev2 & Sev3. Standard errors (SE) in the %AUC values were similar and ranged from 5.2% for the largest %AUC to 9.3% for the smallest %AUC. For further examples of the SE see Table 4.

Stimulus Protocol	AUC (%), All Sev	AUC (%), Sev2 and 3
Photo1	65.8	68.2
Photo1F	80.3	86.2
Photo2	80.8	80.3
Photo2F	**84.1**	**89.1**
Scot1	72.7	75.1
Scot1F	**81.3**	**83.2**
Scot2	64.0	68.6
Scot2F	62.9	57.2

Table 4 details the mean %AUC ± SE values for *Photo2F* and *Scot1F* categorised by disease severity. For Sev3 (exudative AMD) the AUC values for the photopic condition were higher (Sev3: cf. 85.1% and 92.8%) when pattern the deviation (PD) method is employed, whereas in scotopic condition, the AUC values were similar and lower for either the TD or PD method (90.3%). When pooling the Sev2 and 3 eyes the photopically measured PDs performed best (%AUC = 89.1 ± 6.6). That result was assisted by the better performance obtained for the PDs at photopic levels of Sev2 eyes (%AUC 83.8 ± 9.7) (Table 3, bold).

3.2. Mean effects and defects

To examine the average amplitude changes caused by AMD we fitted multivariate linear models to the decibel response amplitudes (Section 2). The linear models allowed us to look at the mean deviations from normal field data independent of other possible confounding effects. The models included a reference condition, which was the mean of the direct pupillary responses of male control subjects. The other fitted factors in the model indicate which of the independent effect(s) significantly changed the response amplitudes relative to the reference value.

Table 5 shows the reference response amplitudes of 3.84 ± 0.68 dB (mean ± SE) in the photopic condition, and in scotopic condition 6.24 ± 0.49 dB. Thus, on average, scotopic responses

Table 4
Percent areas under curve (AUC) for receiver operator characteristic plots (±SE), average of three the worst regions, by AMD severity categories.

Severity category	Photo2F		Scot1F	
	TD	PD	TD	PD
SevAll	77.4 ± 5.9	84.1 ± 6.4	81.3 ± 5.0	79.0 ± 7.1
Sev1	51.5 ± 12.3	54.4 ± 16.2	70.6 ± 15.4	82.7 ± 11.0
Sev2	77.0 ± 9.8	**83.8 ± 9.7**	76.9 ± 8.2	67.8 ± 12.9
Sev2 and 3	81.7 ± 5.5	**89.1 ± 6.6**	83.2 ± 4.2	78.4 ± 7.9
Sev3	85.1 ± 4.8	**92.9 ± 8.0**	90.3 ± 3.5	90.3 ± 5.7

SevAll: All patient eyes, TD: total deviation, PD: pattern deviation.

Table 5
Linear model results.

	Photo2F			Scot1F		
	dB	SE	*p*-Value	dB	SE	*p*-Value
Reference	3.84	0.67	*	6.24	0.48	*
Consensual	−0.15	0.25	0.54	−0.19	0.18	0.30
Female	0.76	0.27	0.004	−0.17	0.19	0.37
AMD	−1.18	0.29	*	−1.26	0.22	*
dB/decade age	−0.07	0.17	0.70	−0.48	0.13	*

* Significant at $p < 0.0001$.

larger than photopic responses. For all severities of AMD patients taken together, the mean response amplitudes were significantly reduced in both the photopic, 1.18 ± 0.17 dB, and scotopic 1.26 ± 0.22 dB conditions (both $p < 0.0001$). The decibel reductions translate to mean response reductions of about 30%. Recall that the AUC analysis presented in Tables 3 and 4 were based on the worst three locations in each field, not the mean deviation across the field (see Fig. 3). There was no significant age effect for the photopic stimulus, but there was a small but significant decline of −0.48 ± 0.13 dB/decade of age in scotopic conditions ($p < 0.0001$). Females had slightly larger responses than males in photopic conditions ($p < 0.004$). Table 5 also indicates that consensual responses were significantly smaller at both light levels by <0.2 dB (3–4%).

We then examined an expanded linear model where additional factors were fitted for each visual field location of normal subjects, and also the mean amplitudes of the deviations caused by AMD at those locations (TDs). The results are thus independent of age, gender and consensual response. The mean per region dB contraction amplitudes for normal subjects in photopic and scotopic conditions are expressed as grey scale plots are shown in Fig. 4A and B. In both cases the temporal visual field responses were larger than nasal responses, consistent with our reports from over 6000 mfPOP fields (Carle, Maddess, et al., 2011). Mean changes in amplitudes observed in combined Sev2 and 3 eyes are shown in Figs. 4C and D. For photopic fields five regions were on average significantly reduced compared to normal ($p < 0.01$, Fig. 4C). The two most significant inner regions were suppressed by −6.14 ± 1.24 dB and −5.36 ± 1.24 dB (both $p < 0.00002$). In the scotopic condition (Fig. 4D) five regions were also significantly reduced ($p < 0.01$), the two most significant regions showing mean suppression of −7.66 and −4.80 dB ($p < 0.00002$). It is these sorts of large deviations that produce the larger AUC values in Table 4. The damage recorded under scotopic conditions appeared to be more centralised.

4. Discussion

The main aim of our study was to compare the diagnostic power of mfPOP responses measured to photopic and scotopic stimuli. The stimuli selected for this study tested the whole of central 60° of each visual field with 24 region/eye, and so provided wide retinal coverage and good signal to noise ratios (Maddess et al., 2009) with which to broadly address the issue of light levels.

Although scotopic conditions on average produced severe centralised defects (Fig. 4D), these did not tend to translate into better diagnostic performance than those obtained for photopic conditions (Fig. 3, Tables 3 and 4). By contrast the (possibly) more diffuse damage measured photopically (Fig. 4C) proved to be more diagnostic, with values for Sev2 and 3 combined reaching 89.1 ± 6.60% AUC. Taken together these outcomes would suggest that the scotopic results are more variable across patients and normal subjects. In other words noise in the responses appears to scale with response size rendering the larger responses no more reliable. The mean effect of AMD across the visual field was not significantly different as a *proportion* of the mean response, being about 70% of the mean response in both cases: photopic −1.18 ± 0.29 dB, scotoptic −1.26 ± 0.22 dB. Mean deviations are particular central field locations reach −7 dB (Fig. 4). The results for age, gender, and consensual responses were within the ranges reported in our previous findings (Bell et al., 2010; Maddess et al., 2009).

A more rapid decline of scotopic visual function might be expected from anatomical studies showing that purely age-related reductions in the density of rods in normal subjects are more dramatic than for cones (Curcio et al., 1993; Gao & Hollyfield, 1992). A greater vulnerability of rods compared with cones has been suggested by many psychophysical and histopathological studies of early AMD (Brown et al., 1986; Brown & Kitchin, 1983; Chen et al., 2004; Hogg & Chakravarthy, 2006; Owsley et al., 2000,

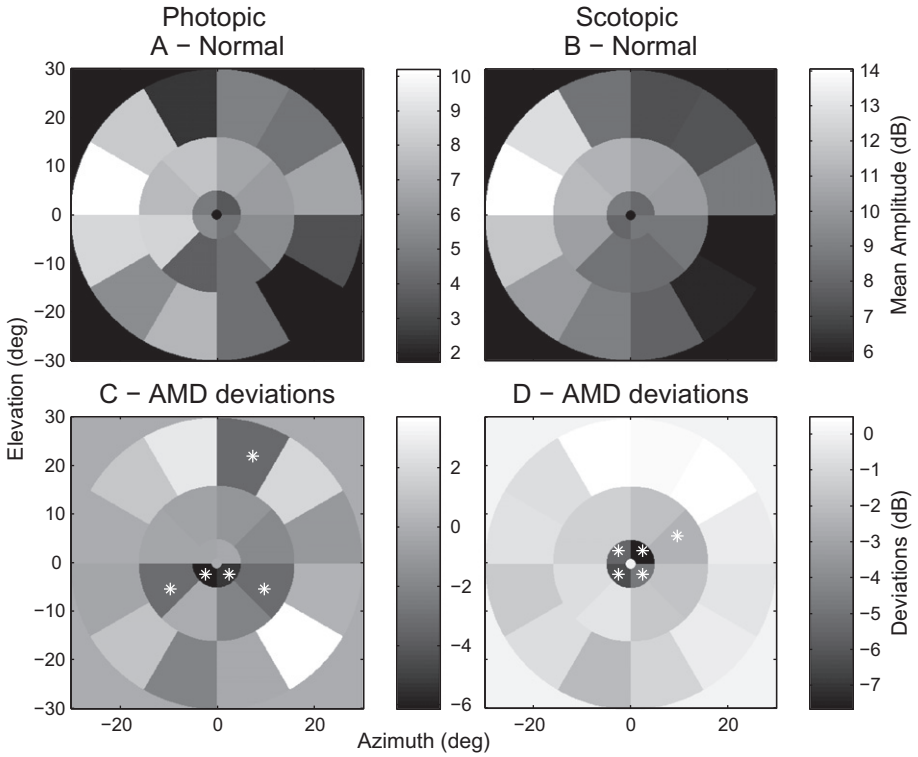

Fig. 4. Mean regional contraction amplitudes of normal subjects under photopic (A) and scotopic (B) conditions. Note the larger scotopic responses. The average deviations from the normal fields (TDs) of all the patient eyes for photopic (C) and scotopic (D) conditions. The average deviations from normality that are significant at the $p < 0.01$ level are indicated by white '*'. Before the regression analysis data from right eyes was flipped left to right so that all data are presented as for left eyes such that the temporal field appears on the left.

2001; Scholl et al., 2004). Certainly few rods have been reported to remain in the parafoveal area in late AMD (Curcio, Medeiros, & Millican, 1996; Madeiros & Curcio, 2001). That being said evidence has been presented that cone condition is linked to that of rods (Chrysostomou, Valter, & Stone, 2009; Leveillard & Sahel, 2010). There is also increasing evidence of early cone damage from ERG studies (Falsini et al., 2000), and the Stiles–Crawford effect suggests changes in foveal cone structure in early AMD (Kanis et al., 2008; Smith, Pokorny, & Diddie, 1988). Those changes may correspond to early changes in the cone cytoskeleton (Eckmiller, 2004), and redistribution of cone-opsin in AMD (Shelley et al., 2009). Recently it has been shown that the recovery of cones from a bleaching flash can produce better sensitivity and specificity than similar rod-based parameters measured in the same early AMD subjects (Dimitrov et al., 2008, 2011, 2012), although mesopic performance may be more important in some high-risk genotypes (Feigl et al., 2011). Flicker thresholds (Dimitrov et al., 2011, 2012) and flicker perimetry (Luu et al., 2012) have shown particular promise in characterising functional loss in early AMD. It was therefore interesting that, of the stimuli tested here, the pedestal flicker stimuli were the most effective here.

The present results suggest that testing in photopic conditions is as good as or better than scotopic testing, at least with the mfPOP method used here. That being said this should be confirmed in the higher resolution mfPOP methods (Sabeti, James, & Maddess, 2011) that have generated better AUC results than here in AMD (Sabeti, Maddess, & James, 2010; Sabeti et al., 2012). New targets for treatment of geographic atrophy have recently been reported (Kaneko et al., 2011), so perhaps devices like mfPOP can have a place in deciding when to treat with current methods, and in future drug development.

Acknowledgments

Financial Support: Australian Research Council (ARC) through the ARC Centre of Excellence in Vision Science (CE0561903), AusIndustry (COM03991), and Seeing Machines Ltd., Canberra.

References

Bell, A., James, A. C., Kolic, M., Essex, R. W., & Maddess, T. (2010). Dichoptic multifocal pupillography reveals afferent visual field defects in early type 2 diabetes. *Investigative Ophthalmology and Visual Science, 51*, 602–608.

Brown, B., Adams, A., Coletta, N., & Haegerstrom-Portnoy, G. (1986). Dark adaptation in age-related maculopathy. *Ophthalmic and Physiological Optics, 6*, 81–84.

Brown, B., & Kitchin, J. (1983). Dark adaptation and acuity/luminance response in senile macular degeneration (SMD). *American Journal of Optometry and Physiological Optics, 60*, 645–650.

Carle, C. F., James, A. C., Kolic, M., Loh, Y., & Maddess, T. (2011). High resolution multifocal pupillographic objective perimetry in glaucoma. *Investigative Ophthalmology and Visual Science, 52*, 604–610.

Carle, C. F., Maddess, T., Kolic, M., Essex, R. W., & James, A. C. (2011). Contraction anisocoria: Segregation, summation and saturation in the pupil light reflex pathway. *Investigative Ophthalmology and Visual Science, 52*, 2365–2371.

Chen, C., Wu, L., Wu, D., Huang, S., Wen, F., Luo, G., et al. (2004). The local cone and rod system function in early age-related macular degeneration. *Documenta Ophthalmologica, 109*(1), 1–8.

Chrysostomou, V., Valter, K., & Stone, J. (2009). Cone-rod dependence in the rat retina: Variation with the rate of rod damage. *Investigative Ophthalmology and Visual Science, 50*(6), 3017–3023.

Curcio, C., Medeiros, N., & Millican, C. (1996). Photoreceptor loss in age-related macular degeneration. *Investigative Ophthalmology and Visual Science, 37*(7), 1236–1249.

Curcio, C., Millican, C., Allen, K., & Kalina, R. (1993). Aging of the human photoreceptor mosaic: Evidence for selective vulnerability of rods in central retina. *Investigative Ophthalmology and Visual Science, 34*(12), 3278–3296.

Curcio, C. A., Owsley, C., & Jackson, G. R. (2000). Spare the rods, save the cones in aging and age-related maculopathy. *Investigative Ophthalmology and Visual Science, 41*(8), 2015–2018.

Curcio, C., Sloan, K., Kalina, R., & Hendrickson, A. (1990). Human photoreceptor topography. *The Journal of Comparative Neurology, 292*(4), 497–523.

Dimitrov, P. N., Robman, L. D., Varsamidis, M., Aung, K. Z., Makeyeva, G., Busija, L., et al. (2012). Relationship between clinical macular changes and retinal function in age-related macular degeneration. *Investigative Ophthalmology and Visual Science,* iovs.11-8958 [pii] 8910.1167/iovs.8911-8958.

Dimitrov, P. N., Guymer, R. H., Zele, A. J., Anderson, A. J., & Vingrys, A. J. (2008). Measuring rod and cone dynamics in age-related maculopathy. *Investigative Ophthalmology and Visual Science, 49*(1), 55–65.

Dimitrov, P. N., Robman, L. D., Varsamidis, M., Aung, K. Z., Makeyeva, G. A., Guymer, R. H., et al. (2011). Visual function tests as potential biomarkers in age-related macular degeneration. *Investigative Ophthalmology and Visual Science, 52*(13), 9457–9469.

Eckmiller, M. S. (2004). Defective cone photoreceptor cytoskeleton, alignment, feedback, and energetics can lead to energy depletion in macular degeneration. *Progress in Retinal and Eye Research, 23*(5), 495–522.

Falsini, B., Fadda, A., Iarossi, G., Piccardi, M., Canu, D., Minnella, A., et al. (2000). Retinal sensitivity to flicker modulation: Reduced by early age-related maculopathy. *Investigative Ophthalmology and Visual Science, 41*(6), 1498–1506.

Feigl, B., Cao, D., Morris, C. P., & Zele, A. J. (2011). Persons with age-related maculopathy risk genotypes and clinically normal eyes have reduced mesopic vision. *Investigative Ophthalmology and Visual Science, 52*(2), 1145–1150.

Gao, H., & Hollyfield, J. G. (1992). Aging of the human retina: Differential loss of neurons and retinal pigment epithelial cells. *Investigative Ophthalmology and Visual Science, 33*(1), 1–17.

Gerth, C. (2009). The role of ERG in the diagnosis and treatment of age-related macular degeneration. *Documenta Ophthalmologica, 118*, 63–68.

Hogg, R. E., & Chakravarthy, U. (2006). Visual function and dysfunction in early and late age-related maculopathy. *Progress in Retinal and Eye Research, 25*(3), 249–276.

Jackson, G. R., Owsley, C., & Curcio, C. A. (2002). Photoreceptor degeneration and dysfunction in aging and age-related maculopathy. *Ageing Research Reviews, 1*(3), 381–396.

James, A. C., Kolic, M., Bedford, S. M., & Maddess, T. (2011). Stimulus parameters for multifocal pupillographic objective perimetry. *Journal of Glaucoma, 21*. http://dx.doi.org/10.1097/IJG.1090b1013e31821e38413.

Kaneko, H., Dridi, S., Tarallo, V., Gelfand, B. D., Fowler, B. J., Cho, W. G., et al. (2011). DICER1 deficit induces Alu RNA toxicity in age-related macular degeneration. *Nature, 471*(7338), 325–330.

Kanis, M. J., Wisse, R. P., Berendschot, T. T., van de Kraats, J., & van Norren, D. (2008). Foveal cone-photoreceptor integrity in aging macula disorder. *Investigative Ophthalmology and Visual Science, 49*(5), 2077–2081.

Kolic, M., Maddess, T., Essex, R. W., & James, A. C. (2010). Effect of intra ocular lens implants on diagnostic performance of multifocal objective perimetry in glaucoma. *ARVO-IOVS,* 51 (pp. E-Abstract 5513).

Leveillard, T., & Sahel, J. A. (2010). Rod-derived cone viability factor for treating blinding diseases: From clinic to redox signaling. *Science Translational Medicine, 2*(26), 26ps16.

Luu, C. D., Dimitrov, P. N., Robman, L., Varsamidis, M., Makeyeva, G., Aung, K. Z., et al. (2012). Role of flicker perimetry in predicting onset of late-stage age-related macular degeneration. *Archives of Ophthalmology, 130*(6), 690–699.

Maddess, T., Bedford, S., Goh, X., & James, A. (2009). Multifocal pupillographic visual field testing in glaucoma. *Clinical and Experimental Ophthalmology, 37*, 678–686.

Maddess, T., Ho, Y. L., Wong, S. S., Kolic, M., Goh, X. L., Carle, C. F., et al. (2011). Multifocal pupillographic perimetry with white and colored stimuli. *Journal of Glaucoma, 20*(6), 336–343.

Madeiros, N., & Curcio, C. (2001). Preservation of ganglion cell layer neurons in age-related macular degeneration. *Investigative Ophthalmology and Visual Science, 42*, 795–803.

Mitchel, P., Smith, W., & Altebo, K. (1995). Prevalence of age-related maculopathy in Australia: The Blue Mountain study. *Ophthalmology, 102*, 1450–1460.

Neelam, K., Nolan, J., Chakravarthy, U., & Beatty, S. (2009). Psychophysical function in age-related maculopathy. *Survey of Ophthalmology, 54*(2), 167–210.

Owsley, C., Jackson, G. R., Cideciyan, A. V., Huang, Y., Fine, S. L., Ho, A. C., et al. (2000). Psychophysical evidence for rod vulnerability in age-related macular degeneration. *Investigative Ophthalmology and Visual Science, 41*(1), 267–273.

Owsley, C., Jackson, G. R., White, M., Feist, R., & Edwards, D. (2001). Delays in rod-mediated dark adaptation in early age-related maculopathy. *Ophthalmology, 108*(7), 1196–1202.

Rosli, Y., Maddess, T., James, A., & Goh, X. (2009). Pattern-pulsed mfVEP waveform of age-related macular degeneration patients. *Akademi Sains Malaysia Science Journal, 3*(1), 31–37.

Sabeti, F., Maddess, T., & James, A. C. (2010). Dichoptic multifocal pupillography identifies retinal dysfunction in early age-related macular degeneration. *ARVO-Investigative Ophthalmology and Visual Science,* 51 (pp. E-Abstract 2794).

Sabeti, F., James, A. C., & Maddess, T. (2011). Spatial and temporal stimulus variants for multifocal pupillography of the central visual field. *Vision Research, 51*, 303–310.

Sabeti, F., Maddess, T., Essex, R. W., & James, A. C. (2011). Multifocal pupillographic assessment of age-related macular degeneration. *Optometry and Vision Science, 88*, 1477–1485.

Sabeti, F., Maddess, T., Essex, R. W., & James, A. C. (2012). Multifocal pupillography identifies ranibizumab induced changes in retinal function for exudative age-related macular degeneration. *Investigative Ophthalmology and Visual Science, 53*, 253–260.

Scholl, H., Bellman, C., Dandekar, S., Bird, A., & Fitzke, F. (2004). Photopic and scotopic fine matric mapping of retinal areas of increased fundus autofluorescence in patients with age-related maculopathy. *Investigative Ophthalmology and Visual Science, 45*, 574–583.

Shelley, E. J., Madigan, M. C., Natoli, R., Penfold, P. L., & Provis, J. M. (2009). Cone degeneration in aging and age-related macular degeneration. *Archives of Ophthalmology, 127*(4), 483–492.

Smith, V. C., Pokorny, J., & Diddie, K. R. (1988). Color matching and the Stiles–Crawford effect in observers with early age-related macular changes. *Journal of the Optical Society of America A: Optics, Image Science, and Vision, 5*(12), 2113–2121.

VanNewkirk, M. R., Nanjan, M. B., Wang, J. J., Mitchell, P., Taylor, H. R., & McCarty, C. A. (2000). The prevalence of age-related maculopathy: The visual impairment project. *Ophthalmology, 107*(8), 1593–1600.